Vol. 16, No. 2, 2025
ISSN 2233-4203/ e-ISSN 2093-8950
ARTICLE www.msletters.org | Mass Spectrometry Letters

Optimizing Collision Energy for Improved Molecular Networking in Non-targeted Lipidomics

Subin Bae[1] and Kwang-Hyeon Liu[1,2]*

[1]*BK21 FOUR Community-Based Intelligent Novel Drug Discovery Education Unit, College of Pharmacy and Research Institute of Pharmaceutical Sciences, Kyungpook National University, Korea*
[2]*Mass Spectrometry Based Convergence Research Institute, Kyungpook National University, Korea*

Received May 4, 2025, Revised June 12, 2025, Accepted June 12, 2025
First published on the web June 30, 2025; DOI: 10.5478/MSL.2025.16.2.64

Abstract : Lipidomics, an emerging field, focuses on the comprehensive analysis of lipid species. However, despite its advances, non-targeted lipidomics approaches continue to encounter significant challenges in lipid annotation, primarily due to the limited coverage of publicly available tandem mass spectrometry spectral libraries. Therefore, this study aims to introduce a non-targeted lipidomics approach using molecular networking to enhance neutral lipid identification. Collision energy conditions were first optimized using commercial neutral lipid standards and subsequently validated with National Institute of Standards and Technology Standard Reference Material 1950 Metabolites in Frozen Plasma. A normalized collision energy of 30, combined with Global Natural Products Social Molecular Networking parameters (cosine score of 0.7 and a minimum of six matched fragment ions), enabled effective spectral connectivity and improved neutral lipid detection. Among the scan ranges tested, the 600–1000 *m/z* range was the most effective, facilitating comprehensive detection of diglycerides, triglycerides, and cholesteryl esters. This study presents an optimized molecular networking strategy for non-targeted lipidomics that enhances both lipid annotation and structural characterization.

Keywords : Non-targeted lipidomics, Molecular networking, Neutral lipids, Collision energy optimization

Introduction

Lipidomics, a specialized field within systems biology, focuses on the comprehensive analysis of lipid molecules to understand their structures, functions, and metabolic pathways. While originally considered a subfield of metabolomics, lipidomics has emerged as a distinct domain within omics sciences. This shift reflects the structural diversity, unique physicochemical properties, and critical biological functions of lipids.[1,2] Recent studies show that lipidomics has further emerged as a key area in systems biology, with broad applications in translational research, including disease diagnosis,[3,4] biomarker discovery,[3] pharmaceutical development,[5] and nutritional assessment of food.[1,6] Lipidomics approaches are generally categorized into targeted[7-10] and non-targeted strategies,[10-12] with analytical methods selected based on the specific aims of the study. Lipids exhibit extensive structural diversity, arising from variations in chain length, saturation, and functional group positions, resulting in thousands of distinct molecular species.[13,14] Owing to this complexity, targeted lipidomics alone is inadequate for comprehensive lipidome profiling, thereby highlighting the complementary role of non-targeted strategies. To address this limitation, non-targeted lipidomics has gained recognition as a promising approach for expanding lipid coverage and facilitating the discovery of novel biomarkers within complex lipid mixtures.

However, lipid annotation in non-targeted lipidomics remains a significant challenge due to the limited availability and coverage of publicly available spectral databases.[15-17] Consequently, < 2% of detected lipid features can be annotated using existing libraries,[15] leaving the substantial portion of lipid species uncharacterized. This highlights a critical limitation of current annotation approaches.

To address this challenge, we propose a non-targeted lipidomics strategy leveraging molecular networking—a key bioinformatics tool for visualizing and annotating chemical diversity in non-targeted mass spectrometry (MS) datasets. Since its introduction in 2012,[18] molecular networking has emerged as an essential method for analyzing non-targeted

*Reprint requests to Kwang-Hyeon Liu
https://orcid.org/0000-0002-3285-5594
E-mail: dstlkh@knu.ac.kr

MS data by grouping structurally related molecules based on spectral similarity. In contrast to conventional reference spectrum-based approaches, molecular networking enables effective visualization and annotation of non-targeted mass spectra without reliance on known spectral libraries.[16,17,19,20,21] Moreover, while molecular networking has shown promise in non-targeted lipidomics, its effectiveness for lipid annotation is hindered by a lack of optimized analytical conditions, limiting its potential for comprehensive lipid profiling.

Therefore, this study aims to optimize molecular networking for the improved annotation of neutral lipids in National Institute of Standards and Technology (NIST®) Standard Reference material (SRM®) 1950 Metabolites in Frozen Plasma as representative real world samples by systematically tuning key MS parameters—specifically collision energy(CE) and MS/MS scan range—as well as Global Natural Products Social Molecular Networking (GNPS) clustering thresholds, using high-resolution MS data. Neutral lipids were selected as the focus of this study because they represent the most abundant class of lipids in the human body and play essential roles in energy storage and metabolic regulation. Optimizing molecular networking for neutral lipid annotation holds potential to advance biomarker discovery and improve the diagnostic utility of non-targeted lipidomics, particularly in complex biological matrices such as plasma. To this end, we employed a data-driven approach integrating high-resolution MS with molecular networking tools to enhance lipid clustering and annotation performance.

Experimental

Reagents and analytical standards

We purchased MS-grade water (H_2O) and methanol (MeOH) from Fisher Scientific Co. (Pittsburgh, PA, USA). Ammonium acetate (NH_4Ac), butylated hydroxytoluene (BHT), chloroform, methyl tert-butyl ether (MTBE), and the NIST SRM 1950 Metabolites in Frozen Plasma were obtained from Sigma-Aldrich (St. Louis, MO, USA). MS-grade isopropanol (IPA) was sourced from Merck (Darmstadt, Germany). Commercial triglyceride (TG) standards were acquired from Avanti Polar Lipids (Alabaster, AL, USA).

Lipid extraction

All lipid extractions from NIST SRM 1950 were performed using the Matyash method with slight modifications.[22] The NIST SRM 1950 was used as a certified human reference sample. A single aliquot (10 μL) was used for extraction, and the material was stored at −80°C until use. As this is a commercially available certified reference material, no additional ethical approval was required. First, 300 μL of ice-cold 100% MeOH containing 0.1% BHT was added to 10 μL plasma, followed by the addition of 90 μL of H_2O. Next, 1 mL of MTBE containing 0.1% BHT was added, and the samples were shaken at room temperature for 1 h. Subsequently, 250 μL of H_2O was added, and the mixture was vortexed for 10 min. Phase separation was conducted through centrifugation at 14,000 × *g* (4°C, 15 min) The supernatant was separated into upper (880 μL) and lower (440 μL) phases. which were then combined. The solvent was evaporated while the dried extract was reconstituted in a total volume of 100 μL, comprising 100 μL of MeOH:chloroform (9:1, *v/v*).

Data-dependent LC–ESI–HRMS/MS analysis

Lipid extracts were analyzed using liquid chromatography-positive electrospray ionization high resolution MS on an Ultimate™ 3000 UHPLC System integrated with a Q Exactive™ Focus Hybrid Quadrupole-Orbitrap™ Mass Spectrometer (Thermo Fisher Scientific Inc., Waltham, MA, USA). Chromatographic separation was performed using a Kinetex® C18 column (100 × 2.1 mm, 2.6 μm; Phenomenex Corporation, Torrance, CA, USA). Lipids were eluted with a binary gradient system comprising 10 mM NH_4Ac in H_2O/MeOH (1:9, *v/v*) as solvent A and 10 mM NH_4Ac in an IPA/MeOH (1:1, *v/v*) as solvent B. The flow rate was maintained at 200 μL/min with the following gradient elution conditions: starting at 30% solvent B, increasing to 95% over 15 min, maintaining 95% for 5 min, and then decreasing to 30% over 5 min. The total analysis time was 25 min. The column oven temperature was set to 40°C, and the injection volume was 1 μL.

The source parameters were as follows: spray voltage, 3500 V; capillary temperature, 320°C, sheath gas flow rate, 40 arb; auxiliary gas flow rate, 2.0 arb; and S-lens RF level, 50. Mass spectral data were obtained using full scan and data-dependent MS/MS ($ddMS^2$) modes. The scan parameters were set as follows: resolution, 70,000; AGC target, 1×10^6 for full scan mode; and resolution, 17,500; AGC target, 5×10^4; maximum injection time, 100 ms; CE and normalized collision energy (NCE), 10–50 eV; and stepped NCE, 15 eV, 30 eV, and 45 eV for $ddMS^2$ mode. For the detection of neutral lipids, the scan range was set to *m/z* 600–1000, based on preliminary evaluations described in the Results section. Chromatographic and spectral data were processed using Xcalibur 4.1 software (Thermo Fisher Scientific Inc., Waltham, MA, USA).

Data preprocessing parameters

Raw data files were converted into the open-source mzXML format with MSConvert 3.0 and subsequently processed using MZmine 2.53. All data processing steps were performed following the guidelines provided in the GNPS documentation.[23] Given that the MZmine parameters for commercial standards were adjusted based on signal intensity, the parameters described below specifically apply to the NIST SRM 1950 samples.

The MS and MS/MS spectra were extracted using

MZmine 2.53, with the mass detection noise levels set at $1E^4$ and $0E^0$, respectively. Chromatograms were constructed using the Automated Data Analysis Pipeline (ADAP) algorithms,[24,25] using a minimum group size of 5 scans, a group intensity threshold of $3E^5$, a minimum peak height of $3E^5$, and an *m/z* tolerance of 5 ppm. The ADAP wavelet-based chromatogram deconvolution algorithm was applied using a baseline cutoff approach with the following parameters: minimum peak height of $3E^5$, baseline level of $1E^5$, peak duration range of 0.1–25 min, *m/z* window for MS/MS scan pairing of 0.01, and retention time (RT) window for MS/MS scan pairing of 0.2 min. Isotopic peaks were grouped using the de-isotoping function with an *m/z* tolerance of 5 ppm and an RT tolerance of 0.1 min. Peak alignment was performed using the join aligner method with the following parameters: *m/z* tolerance of 5 ppm, an absolute RT tolerance of 0.1 min, and weighting factors of 75 and 25 for *m/z* and RT, respectively. Gap filling was conducted using the peak finder module with the following settings: intensity tolerance of 10%, *m/z* tolerance of 5 ppm, and RT tolerance of 0.1 min. Subsequently, the resulting peak list was filtered using the "Feature List Rows Filter" module, requiring a minimum of one peak per row and at least one peak within an isotopic pattern.

Feature-Based Molecular Network Analysis

Molecular networks were constructed using the Feature-Based Molecular Networking (FBMN) workflow on the GNPS platform.[26] The processed MZmine output was evaluated using the FBMN pipeline provided by GNPS. The molecular network was constructed using a precursor ion mass tolerance of 0.02 Da and a fragment ion mass tolerance of 0.02 Da. Nodes were connected when the cosine similarity score exceeded 0.7 and the MS/MS spectra shared at least six matched fragment peaks. Spectral library searches were performed using the same parameter applied during network construction. The resulting molecular networks were visualized and annotated using Cytoscape version 3.4.0 (San Diego, CA, USA).[27]

Lipids annotation in molecular networking

The strategy focused on clusters containing the largest number of nodes. Within these clusters, each node was tentatively annotated using one or more of the following approaches: (1) During molecular network (MN) construction on the GNPS platform, fragment similarity searches were performed across several public databases (e.g. MassBank, HMDB, MoNA). The resulting annotations were automatically incorporated into the MNs generated in Cyto-

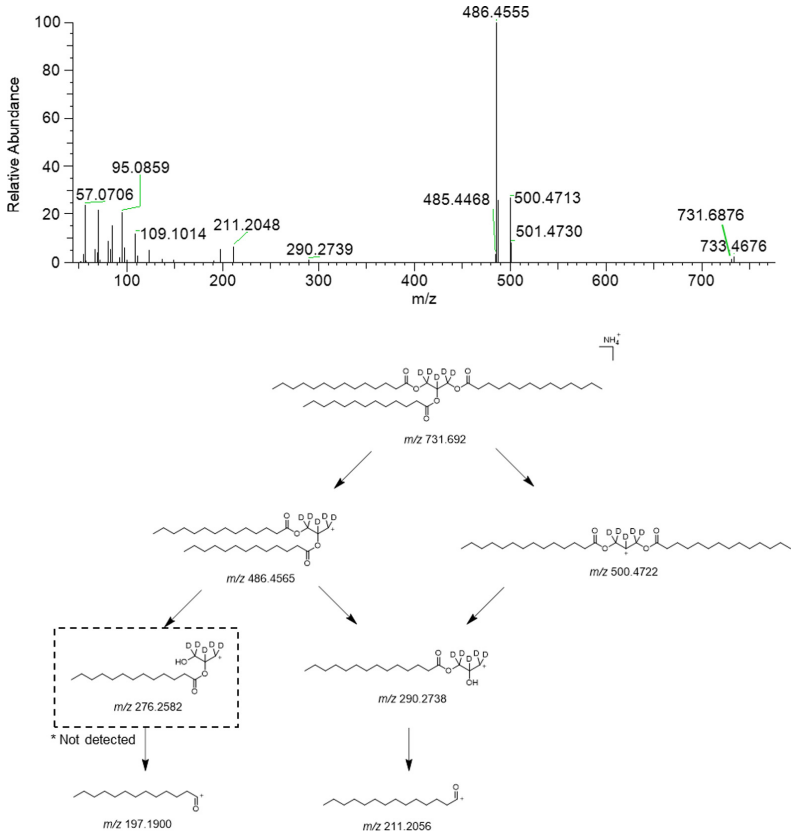

Figure 1. MS/MS spectrum and proposed fragmentation pathway of TG 41:0(14:0/13:0/14:0)-d_5.
Abbreviations: MS/MS, tandem mass spectrometry; TG, triglyceride

scape. (2) The MS data—including accurate mass and fragmentation pattern—were manually compared against entries in other databases such as LIPID MAPS, PubChem, and ChemSpider. (3) When no database matches were found, MS data from all nodes within a cluster were closely analyzed for common fragments ions or neural losses. These shared spectral features were used to infer a possible chemical class, based on literature references or known fragmentation behavior. In each case, once an *m/z* feature was annotated within a cluster, the remaining nodes in that cluster were subsequently annotated based on similarities in their MS/MS spectra and accurate mass differences.

Results and discussion

Fragmentation patterns of neutral lipids

In positive ion mode, TGs are primarily detected as $[M+NH_4]^+$ ions. The observed fragmentation patterns are consistent with those reported in previous studies.[28] For example, Figure 1 illustrates the fragmentation pattern of TG 41:0 (14:0/13:0/14:0)-d_5, featuring fragment ions corresponding to the neutral loss of a 14:0 acyl chain (*m/z* 486.4565) and a 13:0 acyl chain (*m/z* 500.4722). Additional fragment ions due to the loss of two acyl chains were observed at *m/z* 290.2738 and theoretically expected at *m/z* 276.2582, although the latter was not detected in the spectrum. Furthermore, ions corresponding to single fatty acids were observed at *m/z* 197.1900 and 211.2056. All detected fragment ions were within a 5 ppm mass accuracy.

Collision energy optimization for molecular networking

A cosine score (cos) of 0.6 and a minimum of six matched fragment ions (MF) were selected based on widely used settings for molecular networking,[21] with stepped CE applied during analysis. Under these conditions, TGs containing two 14:0 acyl chains were successfully connected, as were those containing two 16:0 acyl chains. However, TGs containing two 18:1 acyl chains did not form any connections (Figure 2a). When the cos threshold was increased to 0.7, the default setting in GNPS, TGs with identical acyl chains were still successfully connected under both stepped NCE and NCE 30 conditions. Furthermore, inter-cluster connections were established, resulting in a single, fully connected network comprising nine TGs (Figure 2b).

These results reflect the fundamental principle that higher *m/z* ions require greater CE for effective fragmentation. While CE settings apply a uniform energy across all *m/z* values, NCE conditions adjust the energy based on the *m/z* value, thereby effectively reducing the energy gap across different ions. This adaptive energy application potentially enhances the connectivity observed in the molecular networks.[29]

Validation using NIST SRM 1950

To identify the optimal CE for neutral lipid analysis and assess the applicability of the optimized conditions to biological samples, the NIST SRM 1950 plasma was used. Various scan ranges (200–1200, 250–850, 300–800, 300–1100, 600–1000, 700–1000) and two CE settings (NCE 30 and stepped NCE) were tested to construct a molecular network and evaluate the suitability of the method for biological sample analysis.

At NCE 30, the scan range of 200–1200 detected 1 diglyceride (DG), 16 TGs, cholesterol, and 9 cholesteryl esters, while the 250–850 range identified 2 monoglycerides (MGs), 5 DGs, 7 TGs, cholesterol, and 9 cholesteryl esters. The 300–800 range detected 2 MGs, 6 DGs, 1 TG, and 9 cholesteryl esters, while the 300–1100 range identified 3 DGs, 18 TGs, cholesterol, and 9 cholesteryl esters. The 600–1000 range detected 6 DGs, 36 TGs, and 9 cholesteryl esters, and the 700–1000 range detected 43 TGs. Under stepped CE, the 200–1200 scan range detected

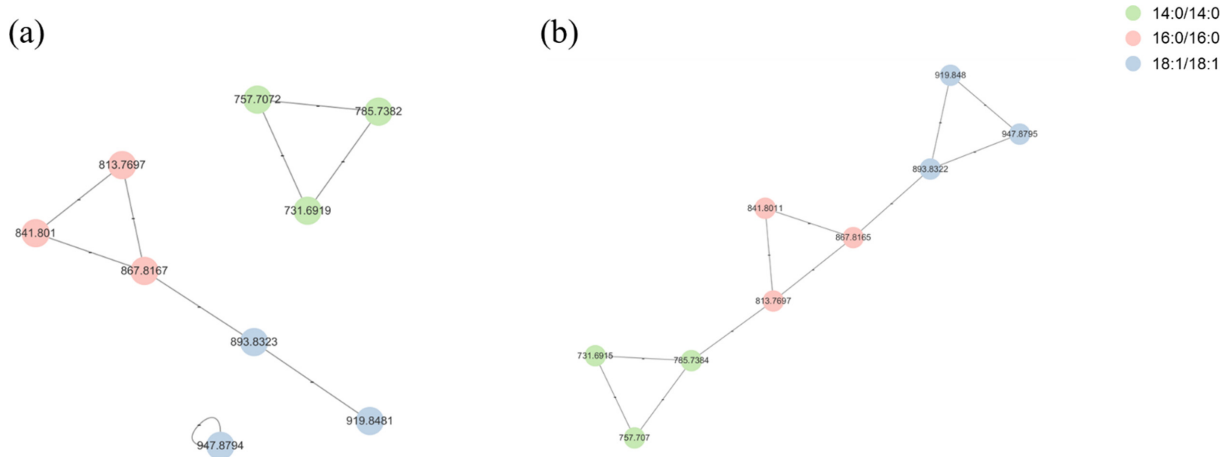

Figure 2. Molecular networks generated using (a) stepped CE (cos: 0.6; MF: 6) and (b) stepped NCE and NCE 30 conditions (cos: 0.7; MF: 6).
Abbreviations: cos, cosine score; MF, minimum fragment ions; CE, collision energy; NCE, normalized collision energy.

10 TGs, while the 250–850 range identified 2 MGs, 5 DGs, and 7 TGs. The 300–800 range detected 1 MG, 5 DGs, and 1 TG, while the 300–1100 range identified 13 TGs. The 600–1000 and 700–1000 ranges detected 6 DGs, 32 TGs, and 35 TGs respectively.

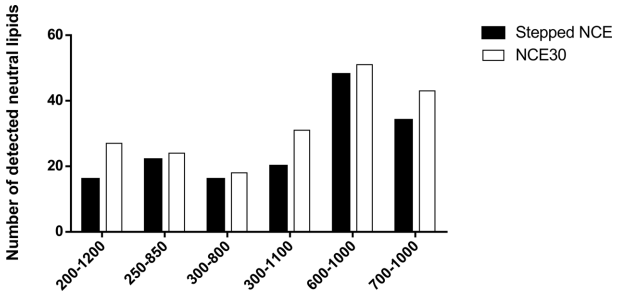

Figure 3. Comparison of neutral lipid detection between NCE 30 and stepped NCE across different scan ranges.
Abbreviations: NCE, normalized collision energy; *m/z*, mass-to-charge ratio

Compared to stepped NCE, the NCE 30 setting consistently detected a broader range of neutral lipids across all tested scan ranges (Figure 3). To further investigate this finding, we compared the variation in neutral lipid detection across different scan ranges under the NCE 30 condition. Furthermore, the 600–1000 scan range was identified as the most suitable for neutral lipid detection, as it facilitated the identification of a diverse range of lipid species, including DGs, TGs, and cholesteryl esters (Table 1). Based on these findings, a molecular network was constructed using the 600–1000 scan range under NCE 30 conditions (Figure 4). Table 2 summarizes the detected neutral lipid species. Consistent with previous studies, 4 of 5 DG species and 30 of 42 TG species were consistently detected in our

Table 1. Neutral lipid species detected across different scan ranges under NCE 30 conditions.

Lipid	Scan range					
	200–1200	250–850	300–800	300–1100	600–1000	700–1000
MG	-	2	2	-	-	-
DG	1	5	6	3	6	-
TG	16	7	1	18	36	43
Cholesterol	1	1	-	1	-	-
Cholesteryl ester	9	9	9	9	9	-

Note: MG, monoglycerides; DG, diglycerides; TG, triglycerides;

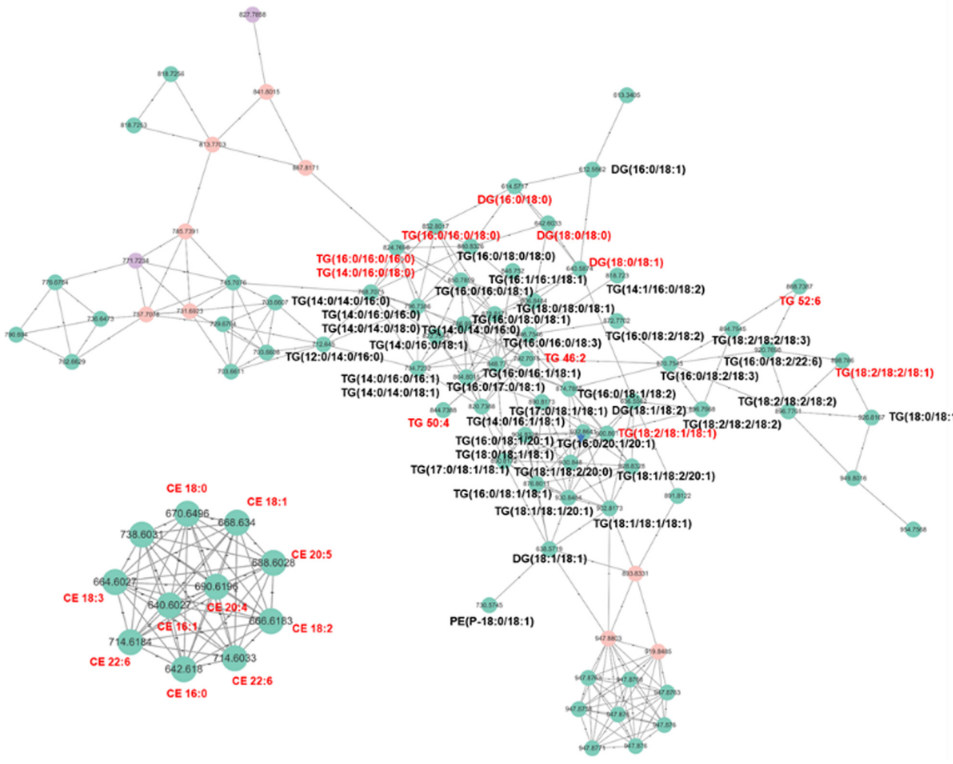

Figure 4. Molecular network of neutral lipids from NIST SRM 1950 constructed using NCE 30 and the 600–1000 scan range.
Abbreviations: NCE, normalized collision energy; *m/z*, mass-to-charge ratio; SRM, Standard Reference Material

Table 2. Neutral lipid species identified from NIST SRM 1950 under NCE 30 conditions using the 600–1000 scan range.

No.		Class	Species	Q_1 (*m/z*)	No.		Class	Species	Q_1 (*m/z*)
1	1	DG	DG 34:1	612.5562	27	21	TG	TG 52:2	876.8011
2	2		DG 34:0	614.5717	28	22		TG 52:1	878.8171
3	3		DG 36:3	636.5562	29	23		TG 52:0	880.8326
4	4		DG 36:2	638.5719	30	24		TG 53:2	890.8172
5	5		DG 36:1	640.5874	31	25		TG 54:7	894.7545
6	6		DG 36:0	642.6033	32	26		TG 54:6	896.7668
7	1	TG	TG 42:0	712.645	33	27		TG 54:5	898.786
8	2		TG 44:1	766.692	34	28		TG 54:4	900.801
9	3		TG 44:0	768.7075	35	29		TG 54:3	902.8173
10	4		TG 46:2	792.7075	36	30		TG 54:2	904.8328
11	5		TG 46:1	794.7232	37	31		TG 54:1	906.8484
12	6		TG 46:0	796.7386	38	32		TG 56:8	920.7698
13	7		TG 48:3	818.723	39	33		TG 56:5	926.8167
14	8		TG 48:2	820.7388	40	34		TG 56:4	928.8328
15	9		TG 48:1	822.7544	41	35		TG 56:3	930.8484
16	10		TG 48:0	824.7698	42	36		TG 56:2	932.8641
17	11		TG 50:4	844.7388	43	1	Cholesteryl ester	Cholesteryl ester 16:1	640.6027
18	12		TG 50:3	846.7546	44	2		Cholesteryl ester 16:0	642.618
19	13		TG 50:2	848.77	45	3		Cholesteryl ester 18:3	664.6027
20	14		TG 50:1	850.7859	46	4		Cholesteryl ester 18:2	666.6183
21	15		TG 50:0	852.8017	47	5		Cholesteryl ester 18:1	668.634
22	16		TG 51:1	864.8015	48	6		Cholesteryl ester 18:0	670.6496
23	17		TG 52:6	868.7387	49	7		Cholesteryl ester 20:5	688.6028
24	18		TG 52:5	870.7545	50	8		Cholesteryl ester 20:4	690.6196
25	19		TG 52:4	872.7702	51	9		Cholesteryl ester 22:6	714.6033
26	20		TG 52:3	874.7855					

Note: DG, diglycerides; TG, triglycerides

analysis. Furthermore, 9 of 15 cholesteryl esters were detected, along with cholesterol, consistent with findings of previous studies.[30] To further confirm the fragmentation consistency, the neutral lipid species detected in the NIST SRM 1950 exhibited fragmentation patterns similar to those observed for TG 41:0(14:0/13:0/14:0)-d_5, including characteristic acyl chain losses and fatty acid ion formation, all within a mass accuracy of 5 ppm.

These findings demonstrate that the combination of NCE 30 with GNPS-recommended parameters (cos of 0.7 and a minimum of six MF ions) most effectively facilitates the detection of the full range of neutral lipids within the 600–1000 *m/z* scan range.

Conclusions

In this study, we optimize the CE conditions for molecular networking-based analysis of neutral lipids. Analysis under the NCE 30 condition, combined with the GNPS-recommended parameters (cos of 0.7 and a minimum of six MF ions), consistently enabled the effective detection of a broad range of neutral lipid species. Among the scan ranges

tested, the 600–1000 *m/z* range was the most suitable for the comprehensive identification of DGs, TGs, and cholesteryl esters. These findings offer a practical framework for enhancing neutral lipid profiling in biological samples and highlight the potential of molecular networking as a potent tool for untargeted lipidomics.

Acknowledgements

The study was conducted with the support of the 2022 Health Fellowship Foundation.

References

1. Sun, T.; Wang, X.; Cong, P.; Xu, J.; Xue, C. *Compr. Rev. Food. Sci. Food. Saf.* **2020**, 19, 2530. https://doi.org/10.1111/1541-4337.12603.
2. Sandra, K.; Sandra, P. *Curr. Opin. Chem. Biol* **2013**, 17, 847. https://doi.org/10.1016/j.cbpa.2013.06.010.
3. Zhao, Y.Y.; Cheng, X.L.; Lin, R.C. *Int. Rev. Cell. Mol. Biol.* **2014**, 313, 1. https://doi.org/10.1016/B978-0-12-800177-6.00001-3.
4. Zandl-Lang, M.; Plecko, B.; Kofeler, H. *Int. J. Mol. Sci.* **2023**, 24. https://doi.org/10.3390/ijms24021709.
5. Lim, S.A.; Su, W.; Chapman, N.M.; Chi, H. *Nat. Chem. Biol* **2022**, 18, 470. https://doi.org/10.1038/s41589-022-01017-3.
6. Yeo, J.; Kang, J.; Kim, H.; Moon, C. *Foods* **2023**, 12. https://doi.org/10.3390/foods12173177.
7. Kwon, Y.J.; Jang, S.N.; Liu, K.H.; Jung, D.H. *Nutrients* **2020**, 12. https://doi.org/10.3390/nu12113423.
8. Kwon, Y.J.; Lee, G.M.; Liu, K.H.; Jung, D.H. *Metabolites* **2021**, 11. https://doi.org/10.3390/metabo11070417.
9. Min, E.K.; Park, S.Y.; Liu, K.H.; Kim, K.T. *J. Hazard Mater.* **2025**, 484, 136712. https://doi.org/10.1016/j.jhazmat.2024.136712.
10. Kim, M.J.; Lee, M.Y.; Shon, J.C.; Kwon, Y.S.; Liu, K.H.; Lee, C.H.; Ku, K.M. *Food Chem.* **2019**, 300, 125169. https://doi.org/10.1016/j.foodchem.2019.125169.
11. Aristizabal-Henao, J.J.; Jones, C.M.; Lippa, K.A.; Bowden, J.A. *Anal. Bioanal. Chem.* **2020**, 412, 7373. https://doi.org/10.1007/s00216-020-02910-3.
12. Nath, L.R.; SG, B.G.; Roberts, T.H.; Gowda, D.; Khoddami, A.; Hui, S.P. *J. Agric. Food Chem.* **2024**, 72, 20690. https://doi.org/10.1021/acs.jafc.4c05919.
13. Koelmel, J.P.; Ulmer, C.Z.; Jones, C.M.; Yost, R.A.; Bowden, J.A. *Biochim. Biophys. Acta Mol. Cell. Biol. Lipids* **2017**, 1862, 766. https://doi.org/10.1016/j.bbalip.2017.02.016.
14. Lee, H.C.; Yokomizo, T. *Biochem. Biophys. Res. Commun.* **2018**, 504, 576. https://doi.org/10.1016/j.bbrc.2018.03.081.
15. da Silva, R.R.; Dorrestein, P.C.; Quinn, R.A. *Proc. Natl. Acad. Sci. USA* **2015**, 112, 12549. https://doi.org/10.1073/pnas.1516878112.
16. Ding, S.; Bale, N.J.; Hopmans, E.C.; Villanueva, L.; Arts, M.G.I.; Schouten, S.; Sinninghe Damste, J.S. *Front. Microbiol.* **2021**, 12, 659315. https://doi.org/10.3389/fmicb.2021.659315.
17. Quinn, R.A.; Nothias, L.F.; Vining, O.; Meehan, M.; Esquenazi, E.; Dorrestein, P.C. *Trends Pharmacol. Sci.* **2017**, 38, 143. https://doi.org/10.1016/j.tips.2016.10.011.
18. Watrous, J.; Roach, P.; Alexandrov, T.; Heath, B.S.; Yang, J.Y.; Kersten, R.D.; van der Voort, M.; Pogliano, K.; Gross, H.; Raaijmakers, J.M.; Moore, B.S.; Laskin, J.; Bandeira, N.; Dorrestein, P.C. *Proc. Natl. Acad. Sci. USA* **2012**, 109, E1743. https://doi.org/10.1073/pnas.1203689109.
19. Nothias, L.F.; Petras, D.; Schmid, R.; Duhrkop, K.; Rainer, J.; Sarvepalli, A.; Protsyuk, I.; Ernst, M.; Tsugawa, H.; Fleischauer, M.; Aicheler, F.; Aksenov, A.A.; Alka, O.; Allard, P.M.; Barsch, A.; Cachet, X.; Caraballo-Rodriguez, A.M.; Da Silva, R.R.; Dang, T.; Garg, N.; Gauglitz, J.M.; Gurevich, A.; Isaac, G.; Jarmusch, A.K.; Kamenik, Z.; Kang, K.B.; Kessler, N.; Koester, I.; Korf, A.; Le Gouellec, A.; Ludwig, M.; Martin, H.C.; McCall, L.I.; McSayles, J.; Meyer, S.W.; Mohimani, H.; Morsy, M.; Moyne, O.; Neumann, S.; Neuweger, H.; Nguyen, N.H.; Nothias-Esposito, M.; Paolini, J.; Phelan, V.V.; Pluskal, T.; Quinn, R.A.; Rogers, S.; Shrestha, B.; Tripathi, A.; van der Hooft, J.J.J.; Vargas, F.; Weldon, K.C.; Witting, M.; Yang, H.; Zhang, Z.; Zubeil, F.; Kohlbacher, O.; Bocker, S.; Alexandrov, T.; Bandeira, N.; Wang, M.; Dorrestein, P.C. *Nat. Methods* **2020**, 17, 905. https://doi.org/10.1038/s41592-020-0933-6.
20. Yu, J.S.; Nothias, L.F.; Wang, M.; Kim, D.H.; Dorrestein, P.C.; Kang, K.B.; Yoo, H.H. *Anal. Chem.* **2022**, 94, 1456. https://doi.org/10.1021/acs.analchem.1c04925.
21. Wang, M.; Carver, J.J.; Phelan, V.V.; Sanchez, L.M.; Garg, N.; Peng, Y.; Nguyen, D.D.; Watrous, J.; Kapono, C.A.; Luzzatto-Knaan, T.; Porto, C.; Bouslimani, A.; Melnik, A.V.; Meehan, M.J.; Liu, W.T.; Crusemann, M.; Boudreau, P.D.; Esquenazi, E.; Sandoval-Calderon, M.; Kersten, R.D.; Pace, L.A.; Quinn, R.A.; Duncan, K.R.; Hsu, C.C.; Floros, D.J.; Gavilan, R.G.; Kleigrewe, K.; Northen, T.; Dutton, R.J.; Parrot, D.; Carlson, E.E.; Aigle, B.; Michelsen, C.F.; Jelsbak, L.; Sohlenkamp, C.; Pevzner, P.; Edlund, A.; McLean, J.; Piel, J.; Murphy, B.T.; Gerwick, L.; Liaw, C.C.; Yang, Y.L.; Humpf, H.U.; Maansson, M.; Keyzers, R.A.; Sims, A.C.; Johnson, A.R.; Sidebottom, A.M.; Sedio, B.E.; Klitgaard, A.; Larson, C.B.; P, C.A.B.; Torres-Mendoza, D.; Gonzalez, D.J.; Silva, D.B.; Marques, L.M.; Demarque, D.P.; Pociute, E.; O'Neill, E.C.; Briand, E.; Helfrich, E.J.N.; Granatosky, E.A.; Glukhov, E.; Ryffel, F.; Houson, H.; Mohimani, H.; Kharbush, J.J.; Zeng, Y.; Vorholt, J.A.; Kurita, K.L.; Charusanti, P.; McPhail, K.L.; Nielsen, K.F.; Vuong, L.; Elfeki, M.; Traxler, M.F.; Engene, N.; Koyama, N.; Vining, O.B.; Baric, R.; Silva, R.R.; Mascuch, S.J.; Tomasi, S.; Jenkins, S.; Macherla, V.; Hoffman, T.; Agarwal, V.; Williams, P.G.; Dai, J.; Neupane, R.; Gurr, J.; Rodriguez, A.M.C.; Lamsa, A.; Zhang, C.; Dorrestein, K.; Duggan, B.M.; Almaliti, J.; Allard, P.M.; Phapale, P.; Nothias, L.F.; Alexandrov, T.; Litaudon, M.; Wolfender,

J.L.; Kyle, J.E.; Metz, T.O.; Peryea, T.; Nguyen, D.T.; VanLeer, D.; Shinn, P.; Jadhav, A.; Muller, R.; Waters, K.M.; Shi, W.; Liu, X.; Zhang, L.; Knight, R.; Jensen, P.R.; Palsson, B.O.; Pogliano, K.; Linington, R.G.; Gutierrez, M.; Lopes, N.P.; Gerwick, W.H.; Moore, B.S.; Dorrestein, P.C.; Bandeira, N. *Nat. Biotechnol.* **2016**, 34, 828. https://doi.org/10.1038/nbt.3597.
22. Matyash, V.; Liebisch, G.; Kurzchalia, T.V.; Shevchenko, A.; Schwudke, D. *J. Lipid. Res.* **2008**, 49, 1137. https://doi.org/10.1194/jlr.D700041-JLR200.
23. GNPS Documentation. https://ccms-ucsd.github.io/GNPSDocumentation/featurebasedmolecularnetworking-with-mzmine2/.
24. Myers, O.D.; Sumner, S.J.; Li, S.; Barnes, S.; Du, X. *Anal. Chem.* **2017**, 89, 8696. https://doi.org/10.1021/acs.analchem.7b00947.
25. Pluskal, T.; Castillo, S.; Villar-Briones, A.; Oresic, M. *BMC Bioinformatics* **2010**, 11, 395. https://doi.org/10.1186/1471-2105-11-395.
26. GNPS Home Page. Available online: http://gnps.ucsd.edu (accessed on 26 May 2020).
27. Shannon, P.; Markiel, A.; Ozier, O.; Baliga, N.S.; Wang, J.T.; Ramage, D.; Amin, N.; Schwikowski, B.; Ideker, T. *Genome Res* **2003**, 13, 2498. https://doi.org/10.1101/gr.1239303.
28. Carriot, N.; Paix, B.; Greff, S.; Viguier, B.; Briand, J.F.; Culioli, G. *Talanta* **2021**, 225, 121925. https://doi.org/10.1016/j.talanta.2020.121925.
29. Thermo scientific Product Support Bulletin. PSB104.
30. Quehenberger, O.; Armando, A.M.; Brown, A.H.; Milne, S.B.; Myers, D.S.; Merrill, A.H.; Bandyopadhyay, S.; Jones, K.N.; Kelly, S.; Shaner, R.L.; Sullards, C.M.; Wang, E.; Murphy, R.C.; Barkley, R.M.; Leiker, T.J.; Raetz, C.R.; Guan, Z.; Laird, G.M.; Six, D.A.; Russell, D.W.; McDonald, J.G.; Subramaniam, S.; Fahy, E.; Dennis, E.A. *J. Lipid. Res.* **2010**, 51, 3299. https://doi.org/10.1194/jlr.M009449.